International Journal of Advanced Structural Engineering (2022) 12 : 665–681

ORIGINAL RESEARCH

Evaluation of Seismic Performance of Multi-Level Pipe Dampers Considering Connection Flexibility in Steel Frames

Mohammad Reza Arabpour [1], Soroush Safakhah [2]*, Ehsan Kazeminezhad [3]

Abstract

The current study is set to investigate the seismic performance of the steel moment-resisting frames equipped with multi-level pipe dampers, considering the connection flexibility in the model. Initially, the behavior model of the damper, connections, and steel columns is presented and calibrated based on the experimental results. Then, three steel moment-resisting frames having 4, 8, and 12 stories with poor lateral strength were modeled in the OpenSees software, while the flexibility of the beam-column connection was taken into account. The structural models were then subjected to a lateral load in one direction and evaluated using nonlinear static analysis. The results revealed that the rehabilitation of steel moment-resisting frames using the multi-level pipe dampers significantly enhanced the load-bearing capacity of the frames compared to the corresponding control frame. The maximum load-bearing capacity increase was 57%, 56%, and 60% in the 4-, 8-, and 12-story frames, respectively. The ultimate deformation capacity increased as well, while the yield displacement of frames decreased. The maximum increase in ultimate ductility of strengthened frames was 43%, 34%, and 33% in the 4-, 8-, and 12-story frames, respectively. The results can be used to compare the performance of this type of damper to that of conventional control structures.

Keywords: moment-resisting frame; seismic rehabilitation, multi-level pipe damper; connection flexibility

1- Introduction

Recently occurring earthquakes have shown that most structures constructed in the past based on old codes of design and construction have not resisted actual earthquake forces, or at least they did not feature a sufficient level of strength [1]. Hence, studying the vulnerability of existing structures and proposing a rehabilitation plan for them that is both technically and economically justifiable is of high importance [2].

✉ Corresponding author: Safakhah@semnaniau.ac.ir

1. Department of Civil Engineering, Semnan Branch, Islamic Azad University, Semnan, Iran
2. Department of Civil Engineering, Semnan Branch, Islamic Azad University, Semnan, Iran
3. Department of Civil Engineering, Ahvaz Branch, Islamic Azad University, Ahvaz, Iran

Cheraghi and Zahraei [3, 4] introduced multilevel pipe-in-pipe steel dampers in 2016 and analyzed them under quasi-static lateral cyclic load. This type of damper is made up of concentric, nested steel pipes connected by pistons. There are gaps between the pipes whose values are determined according to the flexural stiffness of the exterior pipe as well as its length, diameter, and thickness.

Given the recent development of multi-level pipe dampers and the fact that these steel dampers have been evaluated in a limited number of studies for steel structure strengthening purposes, the current study sought to investigate the application of the aforementioned dampers for steel building rehabilitation. On the other hand, almost all research has been carried out on the impacts of multi-level pipe dampers on the seismic behavior of steel buildings without consideration of beam-column connection flexibility. Since the consideration of the nonlinear behavior of connections can significantly affect the lateral responses of the steel moment frames, this paper introduces a novel concept in the strengthening field, the results of which could be widely utilized by the civil engineering community.

1.1. Material models for steel in OpenSees software

The stress-strain relationship for the steel material is assigned using the Steel02 model in OpenSees. This material model was created based on the Menegotto-Pinto stress-strain model (1973) [5], benefiting from the consideration of isotropic and kinematic hardenings. Furthermore, the curvature level of the transition zone from linear to nonlinear phase can be predetermined. The stress-strain behavior of this material is presented in Fig. 1.

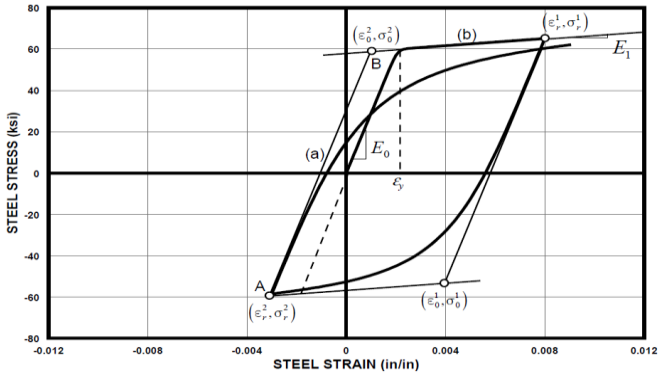

Fig. 1: Menegotto-Pinto stress-strain model for modeling the steel material [5]

The expected yield strength for the steel material is assumed to be 264 MPa; the post-yield hardening of steel is set to 1% of its initial stiffness value, and the module of elasticity for the steel is considered to be 2×10^5 MPa. The isotropic hardening effect was taken into account by substituting values obtained from the experimental results in the model.

1.2. Modeling the steel beam and column elements in OpenSees

To model the members of the steel moment frame, dispBeamColumn nonlinear elements with fiber sections were utilized [5]. Elements are divided into longitudinal strings in this case. Axial stress-strain relations are defined for each string, and general force-displacement relations are computed for each section via the integration of the stress-strain relations of the section's strings [6]. Each column element is divided into five pieces, and each beam element is divided into seven pieces. The number of integration points is five.

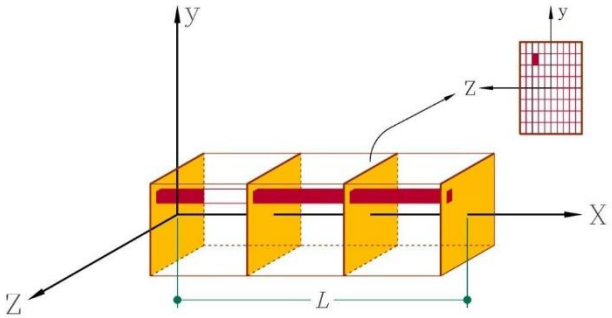

Fig. 2: Member with a fiber section within it

1.2.1. Modeling beam-column connections

Regarding the effect of beam-column connection flexibility on the lateral behavior of steel moment-resisting frames, the aforementioned effect is considered when modeling the steel frames. Various analytical models have been proposed by researchers for modeling beam-column connections. Some analytical models for the simulation of beam-column connections are illustrated in Fig. 3 [1].

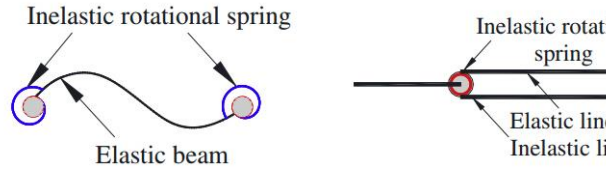

(a) Giberson

(b) Otani

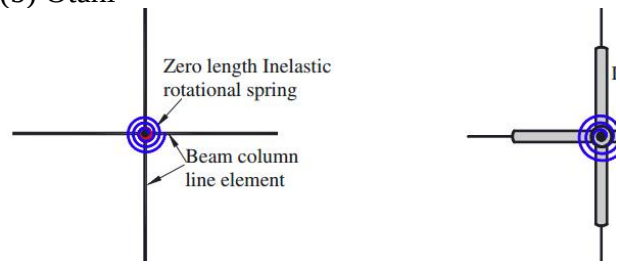

(c) El-Metwally and Chen

(d) Alath and Kunnath

Fig. 3: Different analytical models for simulating steel beam-column connections

To simulate beam-column connections, the model recommended by Alta and Conant, conforming to Fig. 3(c), was used. In this model, deformation resulting from the panel zone can be considered. A zero-length rotational spring element was utilized, and the nonlinear behavior of the connection is assigned according to the experimental results. Pinching4 has a multi-linear pushing response, a loading-unloading trilinear path, and three damage rules assigned to the rotational spring. This behavior model has a wide range of capabilities and can apply various types of produced damages, such as unloading stiffness degradation, reloading stiffness degradation, and strength degradation in different load cycles [7]. Fig. 4 shows the hysteretic model of the Pinching4 material.

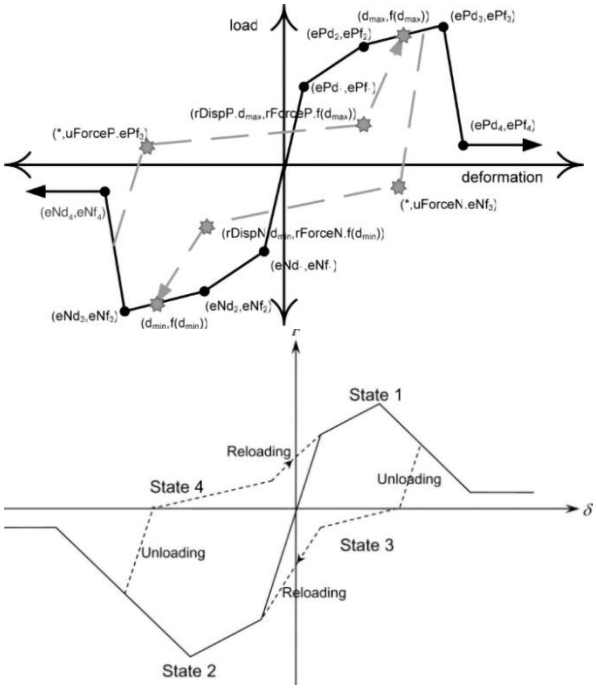

Fig. 4: Hysteretic model of Pinching4 material used in beam-column connection modeling [8]

The load-displacement path for the loading states (statuses 1 and 2) is defined by the pushing curve. During the analysis, the pushing curve can be reformed to consider deterioration in simulation. Status 3 and 4 are also used for the unloading process. Calibration of the models requires 16 parameters that define the push response (status 1 and 2), six parameters to define the two loading-unloading paths (status 3 and 4), and 12 parameters to prescribe the three hysteretic damage rules [4]. Three damage rules used in describing the Pinching4 material model are shown in Fig. 5.

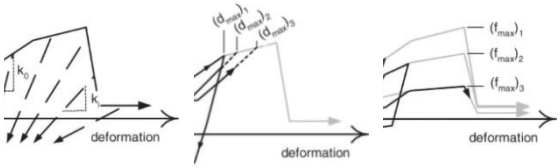

Loading stiffness degradation | **Reloading stiffness degradation** | **Strength Degradation**

Fig. 5: Three damage rules applied in the Pinching4 material model [8]

In the following part, values assigned to these parameters for the steel moment connections are presented. The values required to describe the multi-linear push responses of the Pinching4 model are assigned based on the calibrated force and displacement values that were obtained from the experimental results. Table 1 presents the calibrated parameters for the Pinching4 model applied in a steel beam-column connection.

Table 1: Calibrated parameters for the Pinching4 model applied in beam-column connection

Connection type	rDisp	rForce	uForce
Steel beam-column connection	0.2	0.9	0.55

Where;
rDisp: Ratio of displacement to the maximum displacement demand in reloading
rForce: Ratio of force to the corresponding force of maximum demanded displacement in reloading
uForce: Ratio of strength related to the negative load during unloading to the maximum strength in one-way loading [9].
In Table 2, calibrated parameters for determining the extent of pinching and the level of damage in steel beam-column connections are explained, in which gK1 to gK4 parameters are related to the unloading stiffness degradation and gD1 to gD4 parameters are related to the reloading stiffness degradation.

Table 2: Calibrated parameters for the Pinching models of beam-column

Connection type	Unloading stiffness degradation					Reloading stiffness degradation				
	gK1	gK2	gK3	gK4	Limit	gD1	gD2	gD3	gD4	Limit
Steel beam-column connection	0.6	0	0.09	0	0.6	0.16	0	0.15	0	0.8

1.2.2. Modeling multi-level pipe dampers

Multi-level pipe dampers are connected to the structure using the diagonal bracings (Fig. 6). When the structure is subjected to the lateral force and deformations occur, tensile and compressive forces are formed within these bracings and their relative dampers, so tension and compression in the damper lead to its deformation, which helps the structure dissipate the earthquake energy (Fig. 7).

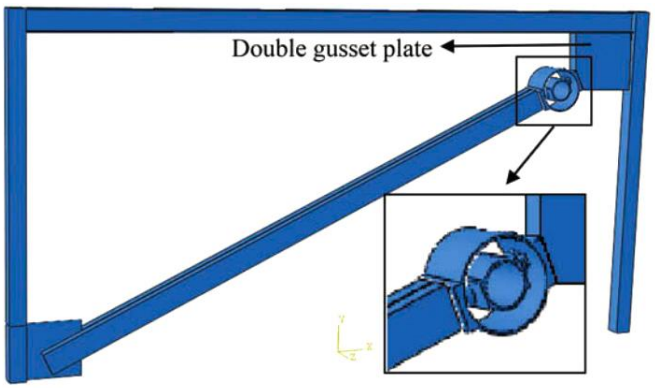

Fig. 6: Location of multi-level pipe damper on the bracing [10]

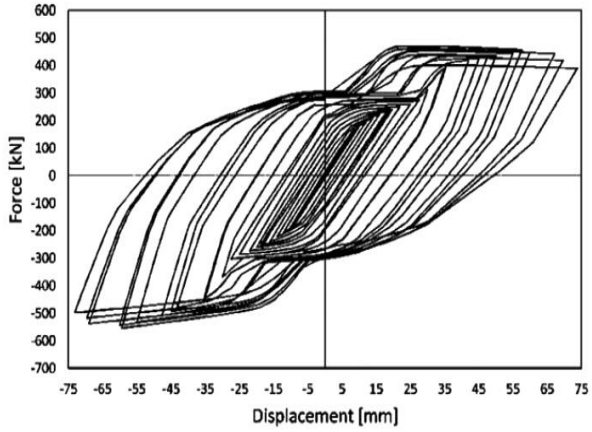

Fig. 7. Hysteretic behavior of damper under tension and compression [10]

A spring (zero-length element) that is able to deform axially under tension and compression was used, and the damper's behavior was assigned to it by means of the Pinching4 model. Multi-linear push response values required to define the Pinching4 model were calibrated based on the experimental results and then assigned. Calibrated parameters of the Pinching4 model for the multi-level pipe damper are presented in Table 3.

Table 3: Calibrated Pinching4 parameter for multi-level pipe damper

Connection type	rDisp	rForce	uForce
Multi-level pipe damper	-0.42	0.45	-0.28

In Table 4, calibrated parameters to determine the extent of pinching in multi-level pipe dampers are proposed.

1.3. Modeling validation in OpenSees Software

1.3.1. Multi-level pipe damper's verification

Cheraghi and Zahraei [3, 4] introduced multi-level pipe in pipe dampers and analyzed them under quasi-static cyclic lateral load. This type of damper is made up of concentric, nested steel pipes connected by pistons. There are gaps between the pipes whose values are determined according to the flexural stiffness of the exterior pipe as well as its length, diameter, and thickness. The main concept of this system was combining various control systems with distinct strength and stiffness values so that the combined system is capable of dissipating energy in a desirable manner when subjected to earthquakes of different intensities (medium to severe). When subjected to a low seismic load, during which the damper deformation is small, a plastic hinge is formed at the exterior pipe, and the input earthquake energy is limited; however, when it is subjected to a severe earthquake, in addition to the exterior pipe, the interior pipe becomes active due to intensified vibrations as well. So, it experiences nonlinear deformations. Thus, strength, stiffness, and the dissipation energy capacity of the system would significantly increase [3]. Fig. 8 illustrates the details of multi-level pipe in pipe damper.

Table 4: Calibrated Pinching4 parameters for multi-level pipe damper

Connection type	Unloading stiffness degradation					Reloading stiffness degradation				
	gK1	gK2	gK3	gK4	Limit	gD1	gD2	gD3	gD4	Limit
Multi-level pipe damper	-0.1	-0.1	10	0.1	-0.32	0.2	0	0.2	0	0.1

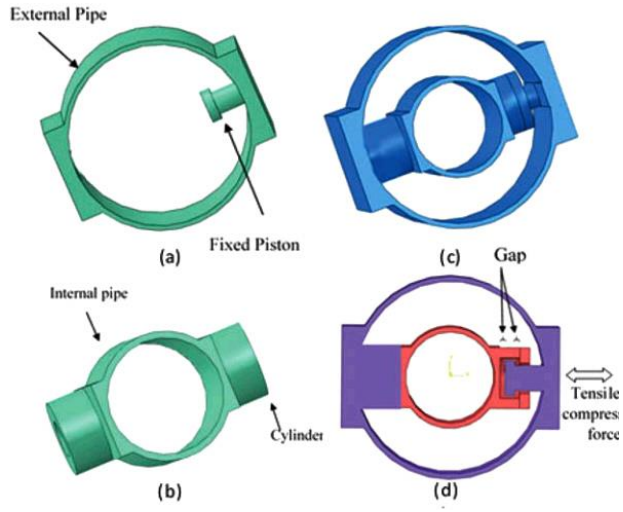

Fig. 8: Multi-level pipe in pipe damper [4]: (a) Exterior pipe; (b) Interior pipe; (c) Assembled damper; (d) Damper's cross section

These researchers constructed two samples of the multi-level pipe in pipe damper that had different geometrical characteristics. Then, they evaluated the samples under a quasi-static cyclic lateral load. The geometrical characteristics of the constructed pipe dampers are presented in Table 5. D_e and D_i parameters represent the exterior pipe diameter and interior pipe diameter, respectively. t_c and t_i parameters are the exterior pipe's thickness and the interior pipe's thickness, respectively. The length of the pipes in both dampers was assumed to be 200 mm.

Table 5: Geometrical characteristics of the examined two-level pipe damper [4]

Sample 1	D_e [mm]	D_i [mm]	t_e [mm]
D.P.S 1	610	320	30
D.P.S 2	400	220	30

The material characteristics of the steel used in the construction of the dampers' pipe are provided in Table 6. It is observed that the plate of damper No. 1 is made of soft steel, while damper No. 2 is made of high-strength steel.

Table 6: Characteristics of the steel material used in the construction of dampers' pipe [4]

Material	Yield stress [MPa]	Ultimate stress [MPa]	Failure strain [%]
Mat 1	295	561	25.2
Mat 2	415	727	20.3

The experimental results by Cheraghi and Zahraei [4] were utilized to validate the analytical models of multilevel pipe dampers. In this regard, pipe damper No. 1, which had already been tested by Cheraghi and Zahraei, was modeled and analyzed under the cyclic load.

Fig. 9 shows the force-displacement hysteretic loops of the multi-level pipe damper No. 1. Part (a) shows the experimental results achieved by Cheraghi and Zahraei, and part (b) indicates the analytical results obtained from the model in OpenSees software.

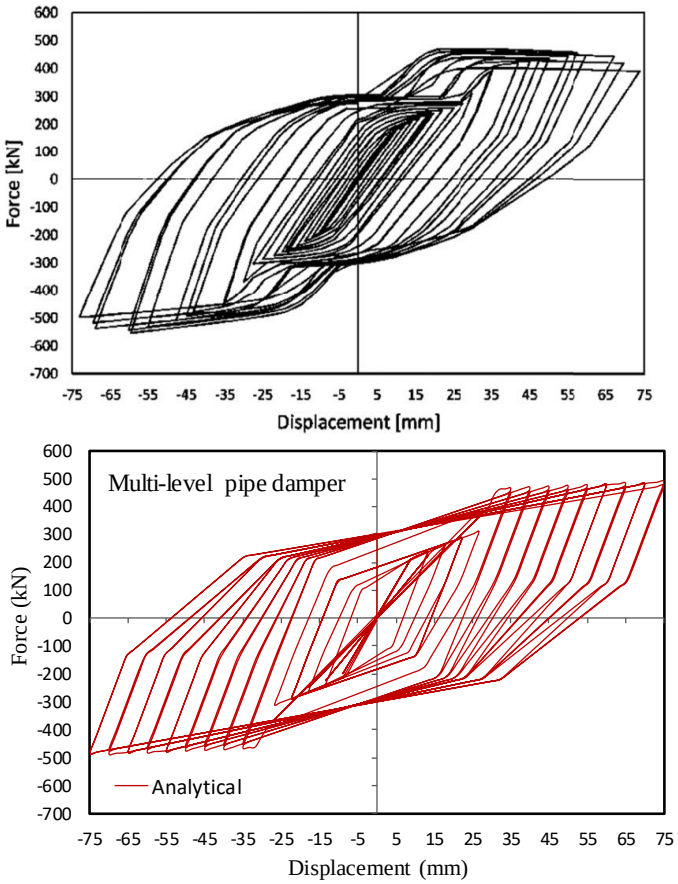

Fig. 9: Force-displacement hysteresis loops of multi-level pipe damper No. 1: (a)

experimental results achieved by Cheraghi and Zahraei; (b) results of OpenSees model

It is observed that the analytical results are in good conformance with the experimental results, and the pinching levels of the hysteresis curves for the two cases are close to each other. The ultimate capacity of the damper in the experimental case is also close to the corresponding value of the analytical model, and the difference is nearly equal to 5%.

Figure 10 depicts the maximum dissipated energy in each cycle for damper No. 1. Part (a) is related to the Cheraghi and Zahraei experimental results, and part (b) belongs to the analytical model created in OpenSees. It is observed that the dissipated energy levels obtained through the enclosed area of the hysteresis loops are in suitable conformance with each other.

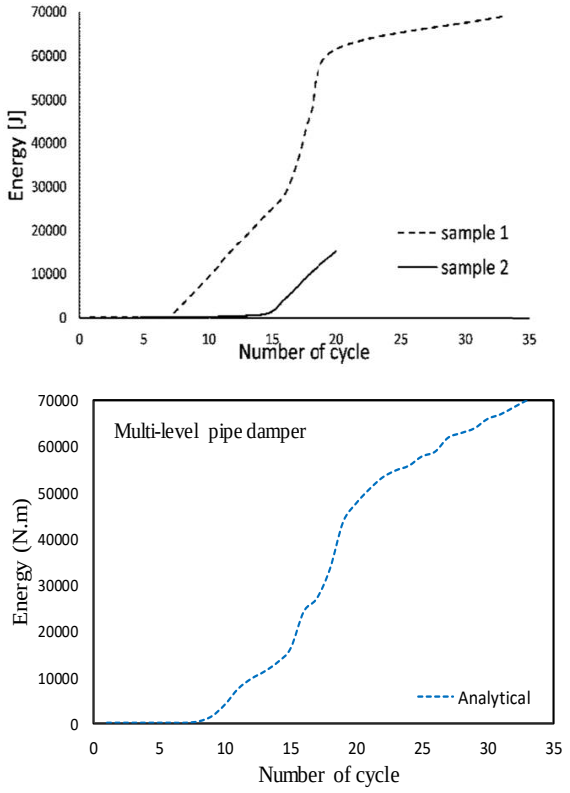

(a)
(b)

Fig. 10: Maximum dissipated energy in each cycle: (a) Cheraghi and Zahraei's experimental results [4]; (b) Analytical results from the OpenSees model

1.3.2. Validation of the steel beam-column connection

To verify the analytical model of steel beam-column connections, a sample of this connection investigated by Yuang et al. [9] was modeled in software. Fig. 11 displays the force-displacement curve for the exterior connection No. 1 (LS1) under the lateral load with increasing amplitude. Part (a) represents the results from Yuang et al.'s experiments, and part (b) is the analytical model obtained from OpenSees.

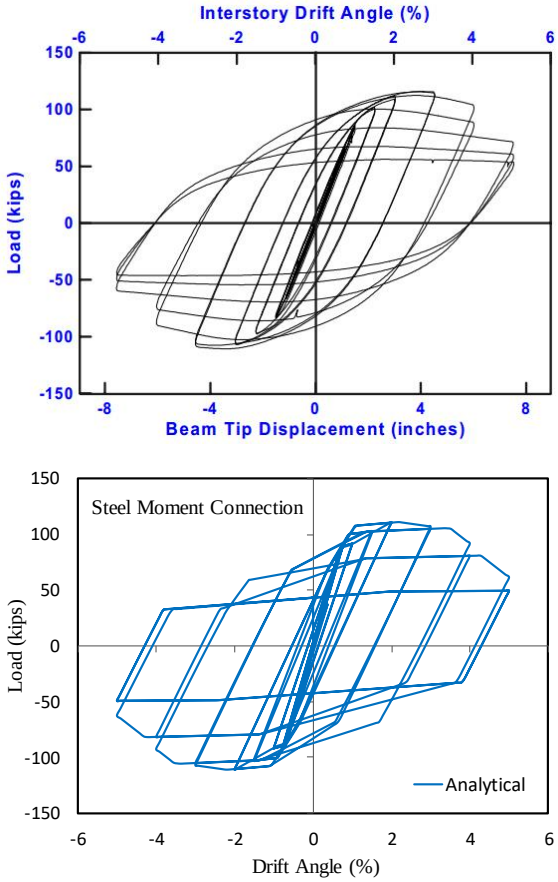

(a)
(b)

Fig. 11: Force-displacement curve of steel connection (LS1): (a) experimental results by Yuang et al. [9]; (b) analytical results from the OpenSees model

It is observed that the experimental results and the analytical model results match well. The maximum strength gained through the experiments is also close in value to the value obtained from the OpenSees model, and the difference is less than 5%. It is observed that the pinching levels of the hysteresis loops are roughly the same.

1.3.3. Validation of steel columns

To verify the analytical model of steel columns, a sample column investigated by Tisuchi et al. [11] was modeled in the software. The target column was subjected to a constant axial load and the lateral cyclic load with increasing amplitude. The ratio of the applied axial load to the axial yield force of the column (N/N_y) was considered to be 0.4, and the lateral load was applied to the column's curvature point in terms of displacement-control load.

The nonlinear element dispBeamColumn, along with the fiber sections, was used in the analytical model of the column. To explore the restraining effects at the column base, a rotational spring of zero length was assumed in the column base. The rotational spring behavior was simulated using Pinching4. The experimental results were also used to calibrate the parameters of Spring. Figure 12 depicts the mathematical model used to simulate the column.

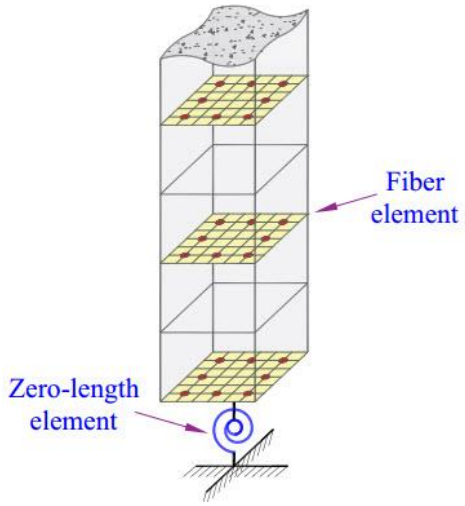

Fig. 12: Analytical model used for simulation of the column [8]

Figure 13 depicts the force-displacement curve of the top of the steel column under constant axial load and lateral increasing load. Part (a) shows the experimental results by Tisuchi et al., and part (b) belongs to the analytical model constructed in OpenSees software.

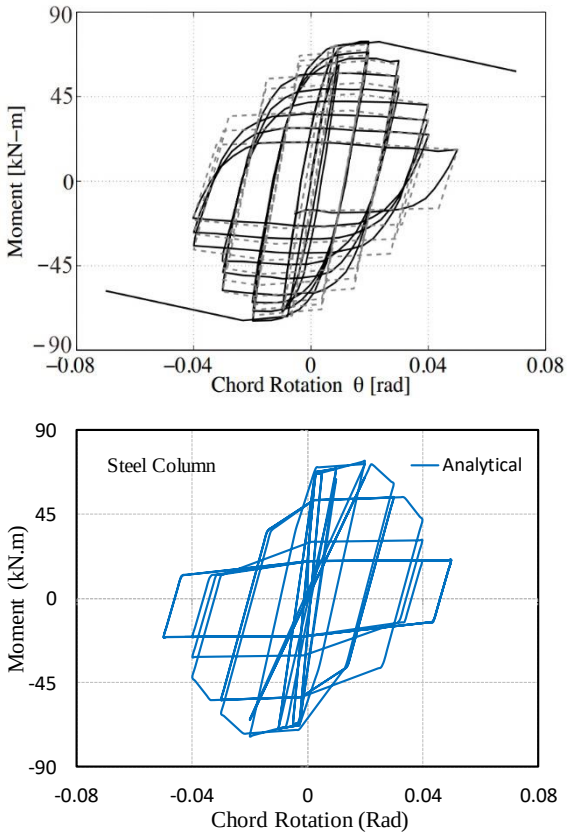

(a)

(b)

Fig. 13: Force- displacement hysteresis curve for the steel column: (a) Experimental results by Tisuchi et al. [12]; (b) Results obtained from the model in OpenSees

A good degree of conformance was observed between the experimental and analytical results. The maximum strength obtained in the analytical model is very close to the corresponding value achieved in the experiments, and the difference in values is less than 5%. It was also observed that the pinching extent of the hysteresis loop in both experimental and analytical cases is roughly comparable.

The validations performed on the columns, steel connections, and multi-level pipe in pipe damper are used to validate the analytical models developed in this study.

1.4. Introducing studied models

Three steel moment frames with four, eight, and twelve stories were modeled in OpenSees software with the beam-column connection flexibility in mind. The above-

mentioned frames were then rehabilitated by the multi-level pipe dampers, and their performance was evaluated to investigate if the lateral behavior of the frames is enhanced or not. To this end, nonlinear static analysis under one-way lateral loading was performed. The frames was designed for 75% seismic base shear conforming to the 2800 Iran standard code (4th edition), since the study was designed to evaluate seismic rehabilitation of steel moment frames. The number of spans in the studied frame is equal to 3, and each span length was considered to be 7 m. The story height for all frames was 3.5 m. It was assumed that the occupancy category of the structures is residential, and they are located in Tehran. Soil type II (based on the 2800 standard soil type classification) was adopted for the models. The medium-strength steel moment-resisting frame with rigid beam and block concrete floor was assumed to be the structural system. The dead load of the stories and the roof was 5 KN/m^2, and the stories' live load and the roof's live load are equal to 2 and 1.5 KN/m^2, respectively [13].

The effective seismic load was considered to be the dead load plus 20% of the live load [6]. The expected yield stress of steel was assumed to be 1.1 times its nominated yield stress, which is 264 MPa [14]. Neglecting the torsional effects, two-dimensional models were utilized. One frame of the structure was extracted and investigated. Fig. 14 shows the plan of the studied structure and the locations of the 4-, 8-, and 12-story extracted frames.

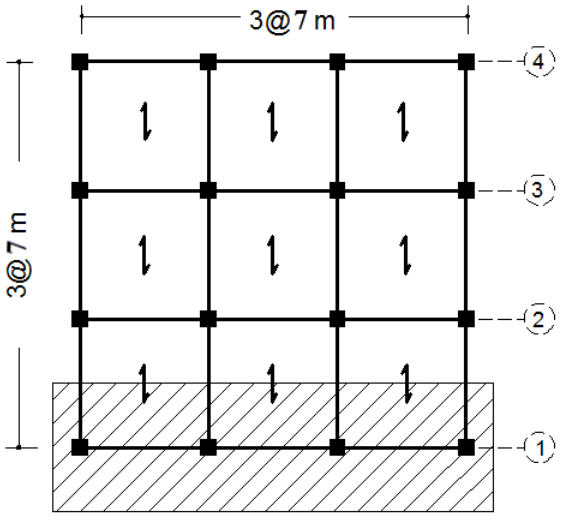

Fig. 14: Plan of structure and location of selected frames

The characteristics of the studied frames and their labeling method are presented in Table 7. Details of 4-, 8-, and 12-story frames' cross sections are also stated in Tables 8 to 10.

Table 7: Labeling of the studied frames

Number of stories	Control frame in poor lateral strength	Rehabilitated frame by the multi-level pipe dampers
Story 4	4S-Control	4S-MPD
Story 8	8S-Control	8S-MPD
Story 12	12S-Control	12S-MPD

International Journal of Advanced Structural Engineering (2022) 12 : 15319–543
https://doi.org/10.1007/s40091-019-00252-8

Table 8: Details of 4-story frame's cross sections

Story	1	2	3	4
Corner column	IPB 220	IPB 220	IPB 180	IPB 180
Center column	IPB 240	IPB 240	IPB 200	IPB 200
Beam	IPE 360	IPE 360	IPE 330	IPE 330

Table 9: Details of 8-story frame's cross sections

Story	1	2	3	4	5	6	7	8
Corner column	IPB 280	IPB 240	IPB 240	IPB 240	IPB 240	IPB 200	IPB 200	IPB 200
Center column	IPB 320	IPB 280	IPB 280	IPB 280	IPB 240	IPB 240	IPB 200	IPB 200
Beam	IPE 360	IPE 360	IPE 360	IPE 360	IPE 360	IPE 330	IPE 330	IPE 330

Table 10: Details of 12-story frame's cross sections

Story	1	2	3	4	5	6	7	8	9	10	11	12
Corner column	IPB 300	IPB 300	IPB 260	IPB 260	IPB 260	IPB 260	IPB 220	IPB 220	IPB 220	IPB 180	IPB 180	IPB 180
Center column	IPB 360	IPB 340	IPB 340	IPB 340	IPB 300	IPB 300	IPB 260	IPB 260	IPB 220	IPB 220	IPB 180	IPB 180
Beam	IPE 400	IPE 400	IPE 400	IPE 360	IPE 360	IPE 360	IPE 360	IPE 360	IPE 360	IPE 330	IPE 330	IPE 330

1.4.1. Design of multi-level pipe dampers

First, the static shear values were calculated to determine the geometrical characteristics of pipe dampers used for frame rehabilitation. Then, the load-bearing capacity of each story's dampers was determined using the damper's geometrical parameters so that the rehabilitated structure could withstand the design shear. To design a multi-level pipe damper, the engineer is engaged with the following parameters: the exterior pipe's diameter (D_e), interior pipe's diameter (D_i), exterior pipe's thickness (t_e), interior pipe's thickness (t_i), damper's length (L), and the gap between the exterior and interior pipe. Selecting the mentioned parameter properly plays a key role in the seismic performance of the damper as well as its absorbed energy. Choosing inappropriate values for these parameters leads to the undesirable performance of dampers. Two types of multi-level pipe dampers are used for strengthening the frames. The diameter and thickness of the exterior pipe in damper type 1 are considered 360 mm and 18 mm, respectively. The diameter and thickness of the interior pipe in the same damper are assumed to be 200 mm and 10 mm, respectively. In damper type 2, the diameter and thickness of the exterior pipe are considered to be 200 mm and 10 mm, respectively. The diameter and thickness of the interior pipe in this damper

are 100 mm and 5 mm, respectively. In all dampers, the ratio of exterior diameter to thickness (D_e/t_e) and the ratio of interior diameter to thickness (D_i/t_i) were presumed to be 20. The ratio of the exterior pipe's diameter to the interior pipe's diameter (D_e/D_i) was presumed to be in the range of 1.8 to 2. The lengths of dampers (L) were mostly decreased or increased instead of changing the diameter or thickness of pipes to achieve a desirable load-bearing capacity as well as energy dissipation in the designed dampers of each story of frames. Characteristics of the designed dampers for 4-, 8-, and 12-story frames are presented in Tables 11 to 13.

Table 11: Geometrical characteristics of the multi-level pipe dampers in the 4-story frame

Story	D_e (mm)	t_e (mm)	D_i (mm)	t_i (mm)	L (mm)	Gsp (mm)	D_e/D_i	D_e/t_e	D_i/t_i	Gap/D_e
1	360	18	200	10	160	25	1.8	20	20	0.07
2	360	18	200	10	145	25	1.8	20	20	0.07
3	360	18	200	10	100	25	1.8	20	20	0.07
4	200	10	100	5	100	18	2	20	20	0.09

Table 12: Geometrical characteristics of the multi-level pipe dampers in the 8-story frame

Story	D_e (mm)	t_e (mm)	D_i (mm)	t_i (mm)	L (mm)	Gsp (mm)	D_e/D_i	D_e/t_e	D_i/t_i	Gap/D_e
1	360	18	200	10	200	25	1.8	20	20	0.07
2	360	18	200	10	200	25	1.8	20	20	0.07
3	360	18	200	10	200	25	1.8	20	20	0.07
4	360	18	200	10	180	25	1.8	20	20	0.07
5	360	18	200	10	150	25	1.8	20	20	0.07
6	200	10	100	5	120	18	2	20	20	0.09
7	200	10	100	5	90	18	2	20	20	0.09
8	200	10	100	5	70	18	2	20	20	0.09

International Journal of Advanced Structural Engineering (2022) 12 : 15319–543
https://doi.org/10.1007/s40091-019-00252-8

Table 13: Geometrical characteristics of the multi-level pipe dampers in the 12-story frame

Story	D_e (mm)	t_e (mm)	D_i (mm)	t_i (mm)	L (mm)	Gsp (mm)	D_e/D_i	D_e/t_e	D_i/t_i	Gap/D_e
1	360	18	200	10	220	25	1.8	20	20	0.07
2	360	18	200	10	220	25	1.8	20	20	0.07
3	360	18	200	10	220	25	1.8	20	20	0.07
4	360	18	200	10	220	25	1.8	20	20	0.07
5	360	18	200	10	220	25	1.8	20	20	0.07
6	360	18	200	10	220	25	1.8	20	20	0.07
7	360	18	200	10	220	25	1.8	20	20	0.07
8	360	18	200	10	160	25	1.8	20	20	0.07
9	360	18	200	10	120	25	1.8	20	20	0.07
10	200	10	100	5	120	18	2	20	20	0.09
11	200	10	100	5	90	18	2	20	20	0.09
12	200	10	100	5	60	18	2	20	20	0.09

1.4.2. Design of braces connected to dampers

Braces connected to dampers are designed to withstand the ultimate generated force in the damper, allowing the braces to remain elastic during earthquakes and preventing buckling [15]. The stiffness of braces to damper stiffness (B/D) ratio and the stiffness of bracings and damper combined to form the story stiffness (SR) ratio should be in the 1 to 2 range. The position of the multi-level pipe dampers in the 4-, 8-, and 12-story restored frames is depicted in Fig. 15. The dampers are installed on the diagonal braces and in the frames' central span.

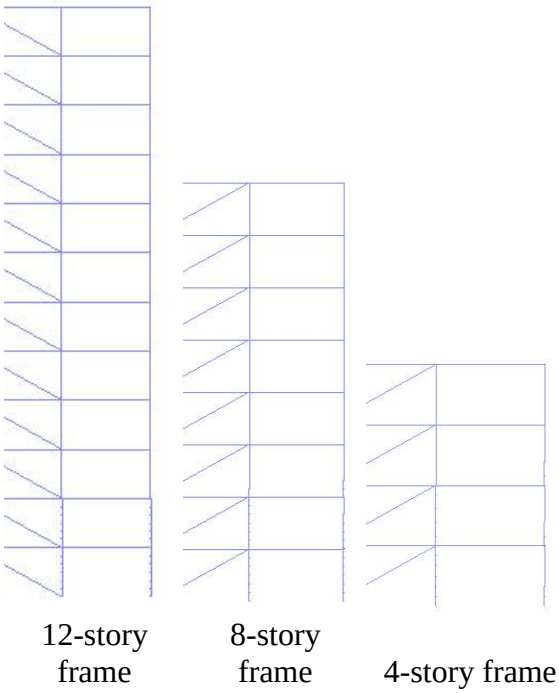

Fig. 15: 4-story, 8-story, and 12-story frames equipped with the pipe dampers

1.5. Results of the analyses

A nonlinear static analysis of all frames was carried out in OpenSees software. For this

purpose, a constant gravity load equal to the dead load plus the effective live load as per ASCE 7-16 [13] was applied to the frames. Regarding the lateral loading, a suitable distribution of lateral forces resulting from the linear dynamic spectrum analysis was considered provided that the mass contribution factor of the structure is equal to or greater than 90% [14]. The P-Δ effects were considered in the analysis as well. In Figs. 15, 16, and 17, the pushover curves of the 4-, 8-, and 12-story control frames are compared with the corresponding curves of the frames rehabilitated with the pipe dampers when they are subjected to the increasing lateral load. When compared to the capacity of the control frame, the lateral load bearing capacity of the frame equipped with dampers is significantly increased. Also, the deformation capacity of the rehabilitated frame is enhanced compared to the control frame's corresponding value. Due to the high initial stiffness of multi-level pipe dampers, it is observed that the initial stiffness of the pushover curves increases when using these dampers. This stiffening can be useful in controlling the lateral displacements of structures during earthquakes.

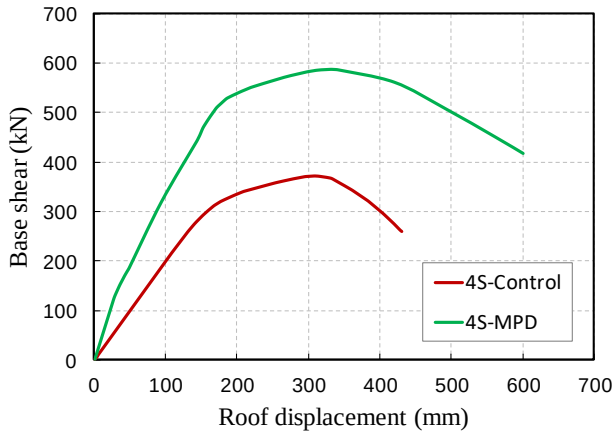

Fig. 16: Comparison between the pushover curve of 4-story control frames and the 4-story frame rehabilitated with the multi-level pipe damper

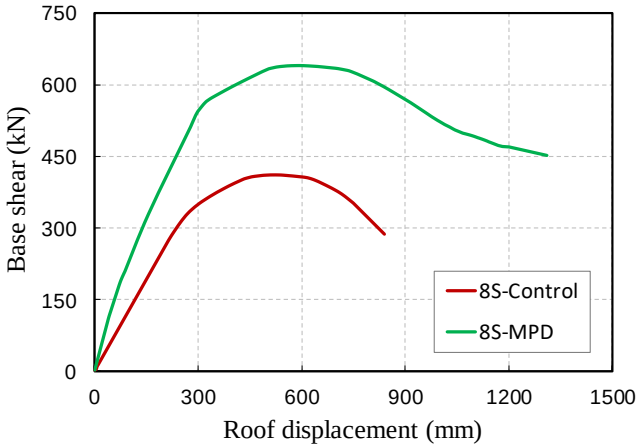

Fig. 17: Comparison between the pushover curve of 8-story control frames and the 8-story frame rehabilitated with the multi-level pipe damper

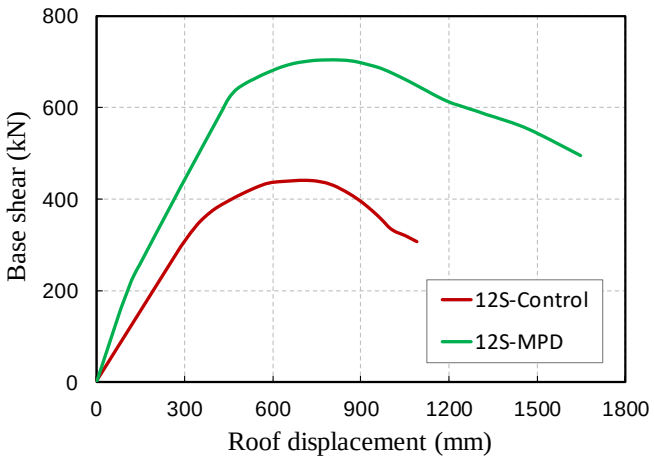

Fig. 18: Comparison between the pushover curve of 12-story control frames and the 12-story frame rehabilitated with the multi-level pipe damper

1.5.1. Lateral load bearing capacity

In Table 14, the maximum lateral load bearing capacities of the 4-, 8-, and 12-story control frames and rehabilitated frames are presented. The percentage increase in the load-bearing capacity of frames equipped with dampers is stated with respect to the corresponding control frames.

International Journal of Advanced Structural Engineering (2022) 12 : 15319–543
https://doi.org/10.1007/s40091-019-00252-8

Table 14: Maximum load bearing capacity of frames

Number of stories	Frame type	P_{max} (kN)	$\frac{P_{max}}{(P_{max})_{Control}}$
Story 4	4S-Control	371.9	1.0
	4S-MPD	584.0	1.57
Story 8	8S-Control	409.2	1.0
	8S-MPD	639.5	1.56
Story 12	12S-Control	438.9	1.0
	12S-MPD	704.2	1.60

The rehabilitation of steel moment frames with multi-level pipe dampers improves the frames' lateral load bearing capacity (Table 14). The maximum load bearing capacity of the 4-story frames equipped with dampers improved by 57% compared to the corresponding control frames, and its value increased from 371.9 KN to 584 KN. The percentage of improvement in load bearing capacity for the 8-story frame is 56%, which shows an increase from 409.2 KN to 639.5 KN. Finally, the percentage of increase in load bearing capacity of a 12-story frame was equal to 60%, which indicates a rise from 438.9 to 704.2 KN.

1.5.2. Ductility

Since the behavior of steel structures is not elastic-perfectly plastic due to the sequence of plastic hinge formation as well as the hardening behavior of the steel material, the force-displacement behavior of frames is transformed to the ideal bilinear curves, and ductility values are extracted from the ideal diagrams. Based on the method suggested by Paulay and Priestley [16], the ideal curve consists of a perfectly elastic branch followed by an elastic branch. The elastic branch is extended from the origin of the curve toward the intersection point with the second branch of the curve (in the range of 70% to 75% of the maximum load value). The following branch or line of the diagram is drawn such that the energy balance (area under the force-displacement curve) is established on both sides of the pushover curve (from the yield point of the member to the point corresponding to a 20% loss in lateral load). In Fig. 19, the procedure for drawing the ideal bilinear curve is shown.

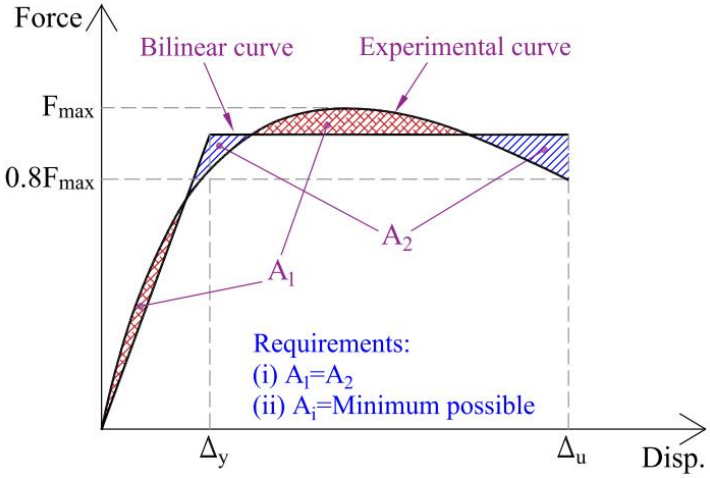

Fig. 19: The ideal bilinear curve for calculation of the yield displacement [8]

Figs. 20–25 presents the ideal bilinear model of 4-, 8-, and 12-story control frames as well as the corresponding rehabilitated frames (equipped with dampers) based on the recommended method by Paulay and Prinestley.

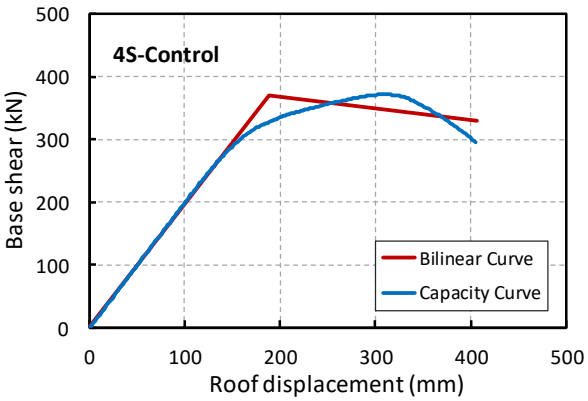

Fig. 20: Ideal bilinear curves for the 4S-control frame

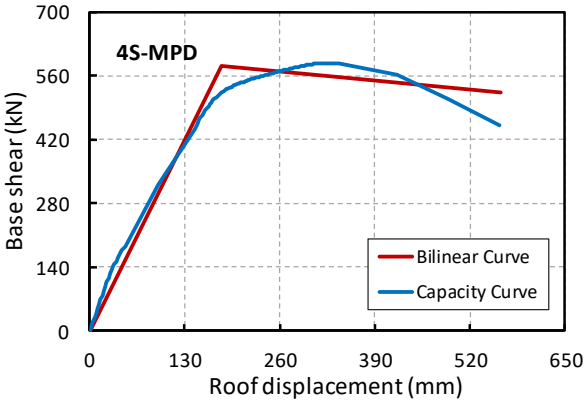

Fig. 21: Ideal bilinear curves for the 4S-MPD frame

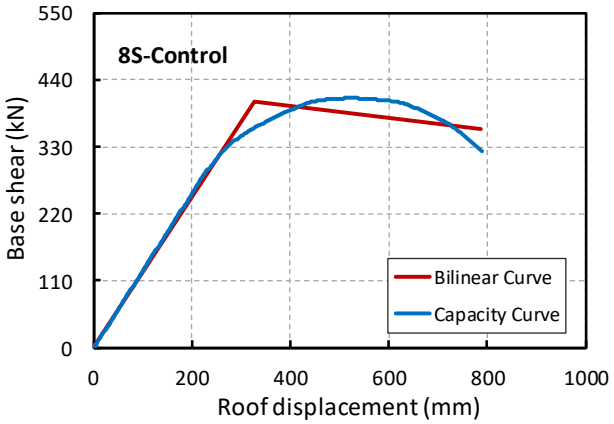

Fig. 22: Ideal bilinear curves for the 8S-control frame

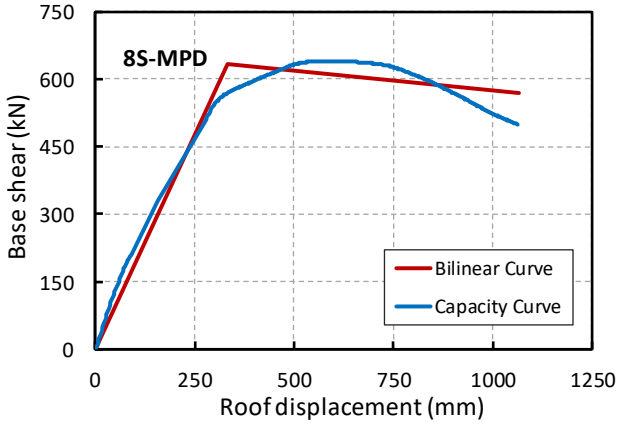

Fig. 23: Ideal bilinear curves for the 8S-MPD frame

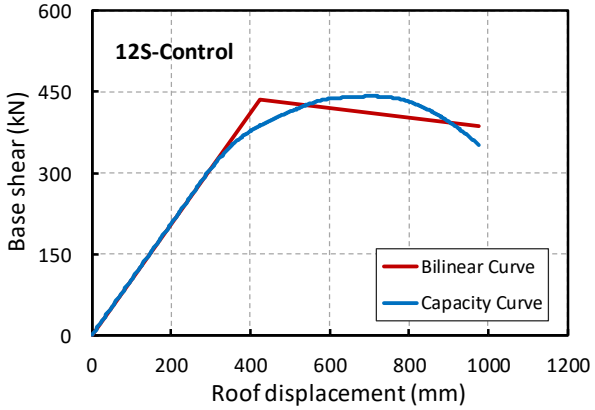

Fig. 24: Ideal bilinear curves for the 12S-control frame

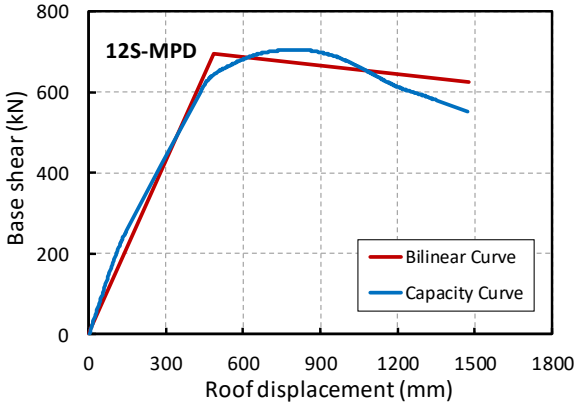

Fig. 25: Ideal bilinear curves for the 12S-MPD frame

In Table 15, the ductility ratios for the 4-, 8-, and 12-story control frames and the respective values for the rehabilitated frames, computed based on equation (4-1), are presented.

$$\mu = \frac{\Delta_u}{\Delta_y} \qquad (4\text{-}1)$$

Where Δ_u denotes the ultimate displacement of frame based on 20% loss in lateral load bearing capacity, and Δ_y represents the yield

displacement of frame based on the bilinear curve.

Table 15: Comparison between the ductility values of control frames and the ductility of frames rehabilitated with the multi-level pipe dampers

Frame type		Δ_y (mm)	Δ_u (mm)	μ	$\frac{\mu}{\mu_{(Control)}}$
Story 4	4S-Control	188	408	2.17	1.0
	4S-MPD	181	562	3.10	1.43
Story 8	8S-Control	329	787	2.39	1.0
	8S-MPD	332	1065	3.21	1.34
Story 12	12S-Control	425	977	2.30	1.0
	12S-MPD	484	1475	3.05	1.33

The results revealed that the ultimate displacement of the rehabilitated frame is greater than the ultimate displacement of the control frame. Furthermore, due to the improved initial stiffness of the frames equipped with dampers, the yield displacement of these frames is reduced. Therefore, the ductility of the rehabilitated frames is significantly enhanced. The ductility of the 4-story rehabilitated frame increased by 43% compared to the corresponding control frame and changed from 2.17 to 3.10. In an 8-story frame, the percentage of change is equal to 34% for the rehabilitated frame (3.21) compared to the control frame (2.39). Finally, the ductility of the 12-story frame changed from 2.30 in the control frame to 3.05 in the rehabilitated frame, which is a 33% increase.

1.6. Conclusion

Considering the effect of connection flexibility, the use of multi-level pipe dampers in the rehabilitation of steel moment frames resulted in a noticeable increase in the lateral load bearing capacity of frames, such that the maximum load bearing capacity of the 4-story frames equipped with dampers improved by 57% compared to the corresponding control frames and its value increased from 371.9 KN to 584 KN. The percentage improvement in load bearing capability for the 8-story frame was 56%, resulting in a jump from 409.2 KN to 639.5 KN. The percentage increase in load bearing capacity of the 12-story frame was equivalent to 60%, indicating a gain from 438.9 to 704.2 KN. The nonlinear static analyses under the one-way lateral load indicated that the rehabilitation of the steel moment frames using the multi-level pipe dampers increased their ultimate deformation capacity and reduced the yield displacement of the frames. In conclusion, the ductility of rehabilitated frames showed a noticeable increase compared to the control frames, such that the ductility of the 4-story rehabilitated frame increased 43% compared to the corresponding control frame, a change from 2.17 to 3.10. In 8-story frame, the percentage of change was equal to 34% for the rehabilitated frame (3.21), compared to the control frame (2.39). The ductility of the 12-story frame changed from 2.30 in the control frame to 3.05 in the rehabilitated frame, which is a 33% increase.

References

[1] Shafaei J, Zareian MS, Hosseini A, Marefat MS. Effects of joint flexibility on lateral response of reinforced concrete frames. Eng Struct 2014;81:412–31. doi:10.1016/j.engstruct.2014.09.046.

[2] Shafaei J, Hosseini A, Marefat MS. Seismic retrofit of external RC beam-column joints by joint enlargement using prestressed steel angles. Eng Struct 2014;81.
[3] Cheraghi A, Zahrai SM. Innovative multi-level control with concentric pipes along brace to reduce seismic response of steel frames. J Constr Steel Res 2016;127:120–35.
[4] Cheraghi A, Zahrai SM. Cyclic testing of multilevel pipe in pipe damper. J Earthq Eng 2017;23:1695–718.
[5] Mazzoni S, McKenna F, Scott M, Fenves G. OpenSees command language manual. Pacific Earthq Eng Res Center, Univ California, Berkeley 2006.
[6] Permanent Committee for revision of Codes. Building seismic design code-Standard 2800 (4th edition). Tehran: Road, Housing & Urban Development Research Center; 1393.
[7] Lowes LN, Altoontash A. Modeling reinforced-concrete beam-column joints subjected to cyclic loading. J Struct Eng 2003;129. doi:/10.1061/(ASCE)0733-9445(2003)129:12(1686).
[8] Seifi A, Hosseini A, Marefat MS, Zareian MS. Improving seismic performance of old-type RC frames using NSM technique and FRP jackets. Eng Struct 2017;147:705–23.
[9] Uang CM, Yu QS, Gilton CS. Effects of loading history on cyclic performance of steel RBS moment connections. Proc 12th WCEE, Up Hutt, New Zeal 2000.
[10] Mualla IH, Belev B. Performance of steel frames with a new friction damper device under earthquake excitation. Eng Struct 2002;24:365–71.
[11] Tsuji B. Inelastic strength and deformation behavior of tubular beam-columns. Proc. Int. Meet. Saf. Criteria Des. Tubul. Struct., 1986, p. 27–35.
[12] Lignos DG, Krawinkler H. Development and utilization of structural component databases for performance-based earthquake engineering. J Struct Eng 2013;139:1382–94.
[13] ASCE/SEI 7-16. Minimum design loads and associated criteria for buildings and other structures. Reston, Virginia: American Society of Civil Engineers (ASCE); 2016.
[14] ASCE/SEI 41-17. Seismic evaluation and retrofit of existing buildings. Reston, Virginia: American Society of Civil Engineers (ASCE); 2017.
[15] Pong W, Vilcheck MG. Design parameters for multi-story structures with damping devices. CTBUH Rev 2001;1.
[16] Paulay T, Priestley MJN. Seismic design of reinforced concrete and masonry buildings. New York: John Wiley & Sons, Inc.; 1992.

International Journal of Advanced Structural Engineering (2022) 12 : 15319–543
https://doi.org/10.1007/s40091-019-00252-8

ORIGINAL RESEARCH